Nitrogen isotope record of a perturbed paleoecosystem in the aftermath of the end-Triassic crisis, Doniford section, SW England

Guillaume Paris, Valérie Beaumont, Annachiara Bartolini, Marie-Emilie Clémence, Silvia Gardin, Kevin Page

Geochemistry Geophysics Geosystems G3

Article
Volume 11, Number 8
26 August 2010
Q08021, doi:10.1029/2010GC003161
ISSN: 1525-2027

Published by AGU and the Geochemical Society

Nitrogen isotope record of a perturbed paleoecosystem in the aftermath of the end-Triassic crisis, Doniford section, SW England

Guillaume Paris
Institut Français du Pétrole, 1&4 rue Bois-Préau, F-92852 Rueil-Malmaison CEDEX, France

Also at Laboratoire de Géochimie-Cosmochimie, Institut de Physique du Globe de Paris, UMR 7579, Université Paris 7, CNRS, Tour 14-24/3E, 4 place Jussieu, F-75252 Paris CEDEX 05, France (paris@ipgp.fr)

Valérie Beaumont
Institut Français du Pétrole, 1&4 rue Bois-Préau, F-92852 Rueil-Malmaison CEDEX, France

Annachiara Bartolini
Département Histoire de la Terre, UMR 5143, Muséum National d'Histoire Naturelle, CNRS, 8 rue Buffon, F-75005 Paris, France

Marie-Emilie Clémence and Silvia Gardin
Centre de Recherche sur la Paléodiversité et les Paléoenvironnements, UMR 7207, UPMC, CNRS, T46-56/5E, case 104, 4 place Jussieu, F-75252 Paris CEDEX 05, France

Kevin Page
School of Geography, Earth and Environmental Sciences, University of Plymouth, Drake Circus, Plymouth PL4 8AA, UK

[1] The Triassic-Jurassic transition (TJ) is characterized by successive perturbations of the carbon cycle during a time of biotic disruption as recorded by the carbon isotopic composition of organic matter ($\delta^{13}C_{org}$). The nitrogen isotopic composition of sedimentary organic matter ($\delta^{15}N_{org}$) constitutes a key parameter to explore the functioning of the ecosystem during carbon cycle perturbations and biological crises, because it provide information on seawater redox conditions and/or nutrient cycling. Here we report the first continuous $\delta^{15}N_{org}$ record across the TJ transition at the Doniford Bay section (Bristol Channel Basin, UK), combined with $\delta^{13}C_{org}$, kerogen typology and carbon ($\delta^{13}C_{min}$) and oxygen ($\delta^{18}O_{min}$) isotopic composition of bulk carbonates. The end Triassic is characterized by a major negative excursion both in $\delta^{13}C_{org}$ and $\delta^{13}C_{min}$, very low TOC (Total Organic Carbon, wt%) and high $\delta^{15}N_{org}$ values, associated with a sea level lowstand. A second $\delta^{13}C_{org}$ negative excursion occurs during the lower Hettangian. This interval is characterized by phases of carbonate production increase alternated with phases of exceptional accumulations of type I organic matter (up to 12%) associated with lower $\delta^{15}N_{org}$ and $\delta^{13}C_{org}$. This alternation likely reflects a succession of nutrient input increase to the basin leading to enhanced productivity and eutrophication, which promoted a primary production driven by organic-walled prokaryotic organisms. The following OM export increase generates anaerobic conditions within the basin. These events occur between periods of relatively good seawater column ventilation and nutrient recycling boosting the carbonate producer recovery. Ecosystems remain perturbed in the Bristol Channel Basin during the aftermath of the end-Triassic crisis.

Components: 9000 words, 5 figures.

Keywords: Triassic-Jurassic boundary; nitrogen isotopes; organic matter; anoxic event.

Index Terms: 1030 Geochemistry: Geochemical cycles (0330); 0469 Biogeosciences: Nitrogen cycling; 1041 Geochemistry: Stable isotope geochemistry (0454, 4870).

Received 1 April 2010; **Revised** 14 June 2010; **Accepted** 18 June 2010; **Published** 26 August 2010.

Paris, G., V. Beaumont, A. Bartolini, M.-E. Clémence, S. Gardin, and K. Page (2010), Nitrogen isotope record of a perturbed paleoecosystem in the aftermath of the end-Triassic crisis, Doniford section, SW England, *Geochem. Geophys. Geosyst.*, *11*, Q08021, doi:10.1029/2010GC003161.

1. Introduction

[2] The late Rhaetian crisis is recognized as one of the "big five" extinction events [*Raup and Sepkoski*, 1982] and the early Jurassic is associated with a time of recovery in an environment that remains perturbed [*Twitchett and Barras*, 2004; *Mander et al.*, 2008; *Clémence et al.*, 2010]. A pronounced sea level fall during the late Rhaetian followed by a rapid sea level rise in the earliest Hettangian (Pre-planorbis beds [*Hesselbo et al.*, 2004] is recognized across Europe [*Hallam and Wignall*, 1999]. The Triassic-Jurassic boundary (TJB) is also marked by the emplacement of the Central Atlantic Magmatic Province (CAMP), one of the most important magmatic provinces of the Phanerozoic [*Courtillot*, 1994; *Marzoli et al.*, 2004; *Nomade et al.*, 2007].

[3] The carbon isotope record at the Triassic-Jurassic transition suggests high instability and successive perturbations of the carbon cycle during a time of biotic disruption in both marine and terrestrial realms [*Ward et al.*, 2001; *Hesselbo et al.*, 2002; *Guex et al.*, 2004; *Hesselbo et al.*, 2004; *Kürschner et al.*, 2007; *Hesselbo et al.*, 2007; *Pálfy et al.*, 2007; *Tomašových and Siblik*, 2007; *Williford et al.*, 2007]. Sea level variations impact the surface of continental margins where the carbonate factory is essentially located in the early Mesozoic and have been suggested as a trigger of the TJ biological crisis [*Hallam*, 1992]. Despite this influence of sea level variations on the carbon cycle, the global $\delta^{13}C$ signal perturbations cannot be interpreted as the consequence of a mere sea level fall. The CAMP emplacement together with methane release was invoked as the main triggers of the crisis [*Pálfy et al.*, 2001; *Beerling and Berner*, 2002; *Hesselbo et al.*, 2004]. Indeed, the CAMP paroxysmal phase has been shown to last between 200 ka and 500 ka close to the end-Triassic mass extinction [*Knight et al.*, 2004; *Cirilli et al.*, 2009; *Schoene et al.*, 2010]. The consequences of large igneous province activity on the biosphere and the carbon cycle are thought to be linked to changes in atmosphere chemical composition, mainly SO_2 and CO_2 input [*Wignall*, 2001a; *McHone*, 2002; *Guex et al.*, 2004; *van de Schootbrugge et al.*, 2009]. The way CAMP emplacement impacts carbon cycle and marine environments is a challenging question investigating the relationships between atmospheric composition and ecosystems functioning.

[4] Recent studies focused on the palaeo-ecology of the marine ecosystem combined with geochemical parameters to try to shed light on the patterns and mechanisms of the Triassic-Jurassic biotic and environmental perturbations [*Barras and Twitchett*, 2007; *van de Schootbrugge et al.*, 2007; *Mander et al.*, 2008; *Clémence et al.*, 2010; M.-E. Clémence et al., Bentho-planktonic evidence of end-Triassic sea-surface carbonate production decline in Austrian Alps, submitted to *Swiss Journal of Geosciences*, 2010]. According to micropaleontological data, *Clémence et al.* [2010] show that immediately after the end Triassic crisis, the carbonate pump recovery in the Bristol Channel Basin seems interrupted by episodic phases of anoxic events. Nitrogen isotopic composition of sedimentary organic matter ($\delta^{15}N_{org}$) provides information on seawater redox conditions, nitrogen metabolism in the basin and/or continental versus marine organic matter (OM) contribution [*Peters et al.*, 1978; *Sephton et al.*, 2002]. These data thus constitute a key parameter to explore the functioning of the ecosystem during carbon cycle perturbations and biological crises. Hereafter, we explore the $\delta^{15}N_{org}$ signal from the Rhaetian-Hettangian transition in the Doniford section (Somerset, England) at high resolution. We present a continuous $\delta^{15}N_{org}$ record across the Triassic-Jurassic transition together with Rock-Eval (RE) data, carbon isotopic composition of organic matter ($\delta^{13}C_{org}$) oxygen and carbon isotopic compositions of carbonates ($\delta^{18}O_{min}$ and $\delta^{13}C_{min}$), and micropaleontological data [*Clémence et al.*, 2010].

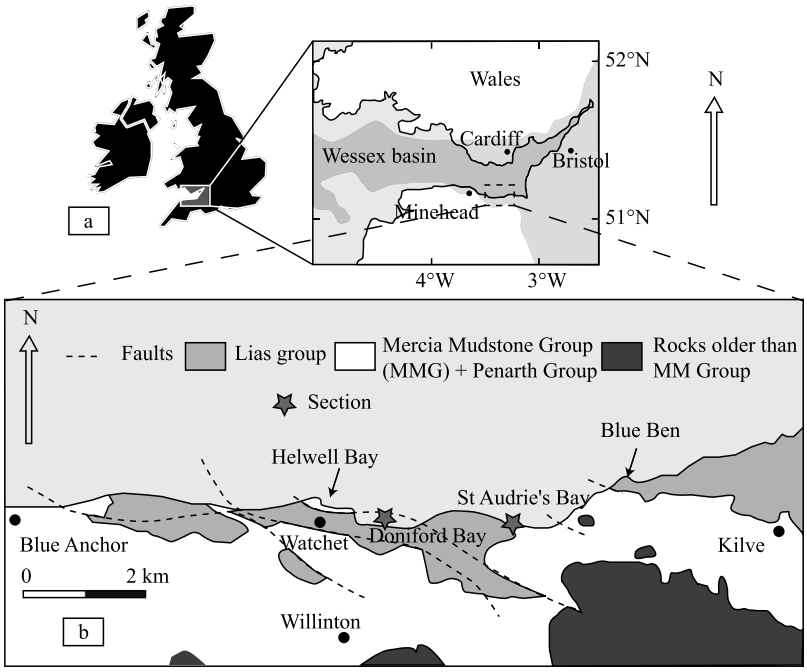

Figure 1. Location of the Doniford section with respect to St Audrie's bay section and Somerset northern coast [*Hounslow et al.*, 2004].

Together with sedimentological information, this data set highlights changes in sea level variations, redox state modifications, changes in nutrient availability and primary producers, food-chain structure (or complexity) in the Bristol Channel Basin across the TJB carbon cycle perturbations.

2. Doniford Section: Lithological and Sedimentological Information

[5] Late Triassic and Early Jurassic marine strata are well exposed on the west Somerset coastline (southern England, Figure 1), between Blue Ben [ST 110440] and Watchet (Helwell Bay) [ST 083433]. Doniford Bay is located about 1 km eastern of Watchet harbor and 2 km western of St Audrie's Bay [*Whittaker and Green*, 1983]. The section is located on the foreshore of the Watchet fault, in the western part of the Doniford Bay [ST 0765 4362]. The late Triassic and early Jurassic sediments (nearly 200 m thick) of SW England are laid down as a succession of east-west extensional basins (Figure 1b). Rhaetian conditions are essentially marine [*Hesselbo et al.*, 2004]. A sea level rise is observed, culminating with a Maximum Flooding Surface during the deposition of the late Rhaetian Westbury Formation (Figure 2). Dark gray mudstones including limestone horizons are deposited in this offshore setting. The overlying Lilstock Fm (formation) is marked by a sea level fall during the time of deposition of the Cotham Member (below the Langport Member), corresponding to an inner-shelf tidal environment, and lowstand dominates during the Langport Member deposition. Lithologies of the sampled part of the stratigraphic succession, above the Cotham Member, are reported in Figure 2. A rapid sea level rise occurs during the early Hettangian and outer-shelf marine environments are maintained in the area through the early Jurassic (Lias Group) marked by the alternation of

Figure 2. Stratigraphical and lithological logs of the Doniford section. (a) Mineral carbon content ($CaCO_3$ wt%); carbon and oxygen isotopic composition (versus PDB ‰). (b) Organic carbon content (TOC, wt%); carbon and nitrogen isotopic composition (versus PDB and AIR, respectively, ‰). (c) RE-based redox conditions (column 1); comparison with micropaleontological data: nannofossils and organic walled organisms (column 2); benthic foraminifers abundance peaks (column 3). See auxiliary material. Closed circles (resp. open) are for samples with HI > 650 (resp. HI < 650) mgHC/gTOC.

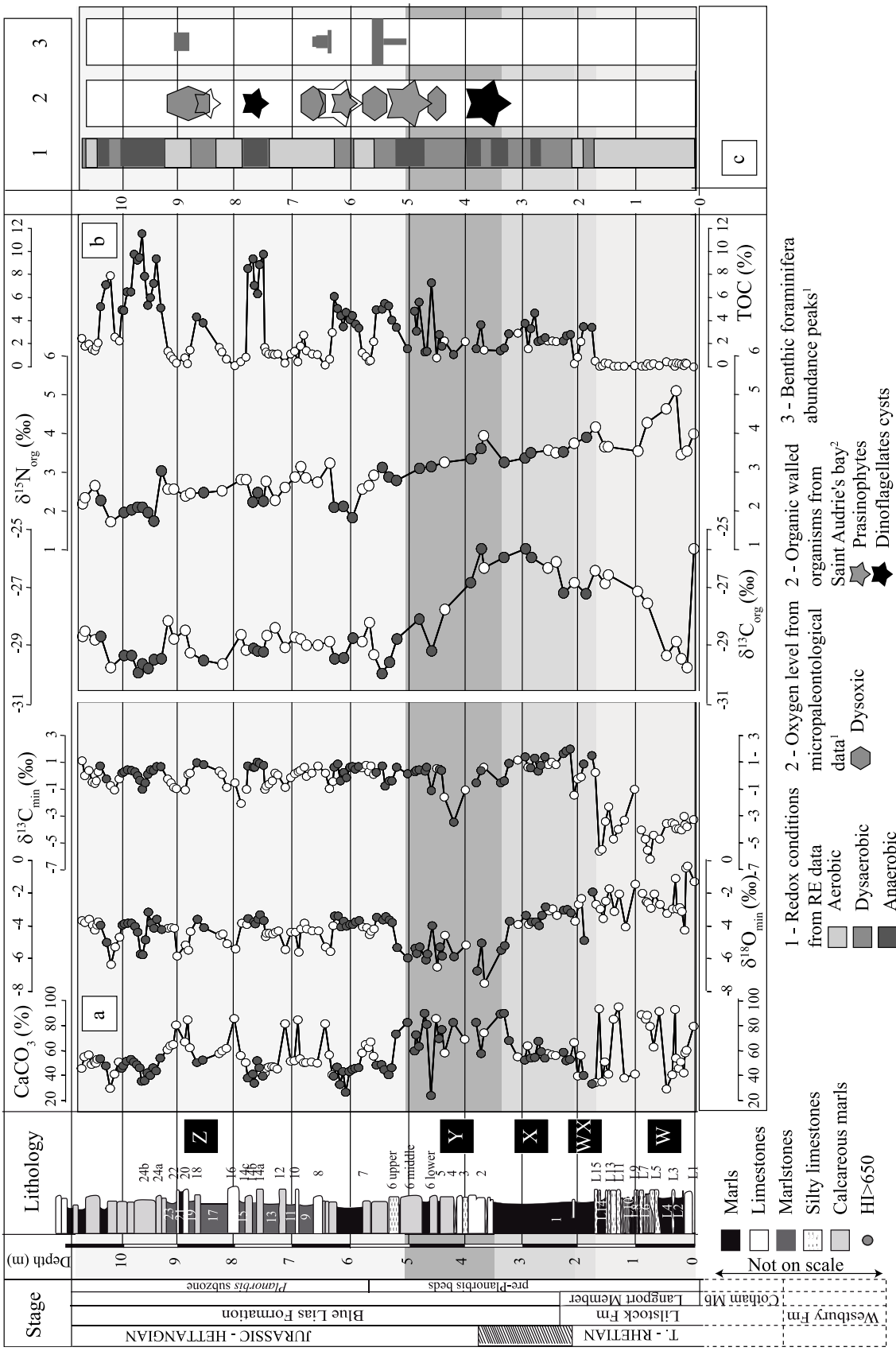
Stage
Lithology
Depth (m)
Not on scale
JURASSIC - HETTANGIAN
T. - RHETTIAN
Blue Lias Formation
Lilstock Fm
Langport Member
Cotham Mb
Westbury Fm
pre-Planorbis beds
Planorbis subzone
Marls
Limestones
Marlstones
Silty limestones
Calcareous marls
HI>650
CaCO3 (%)
δ18Omin (‰)
δ13Cmin (‰)
δ13Corg (‰)
δ15Norg (‰)
TOC (%)
a
b
c
1 - Redox conditions from RE data
Aerobic
Dysaerobic
Anaerobic
2 - Oxygen level from micropaleontological data1
Dysoxic
2 - Organic walled organisms from Saint Audrie's bay2
Prasinophytes
Dinoflagellates cysts
Acritarchs
3 - Benthic foraminifera abundance peaks1

Figure 2

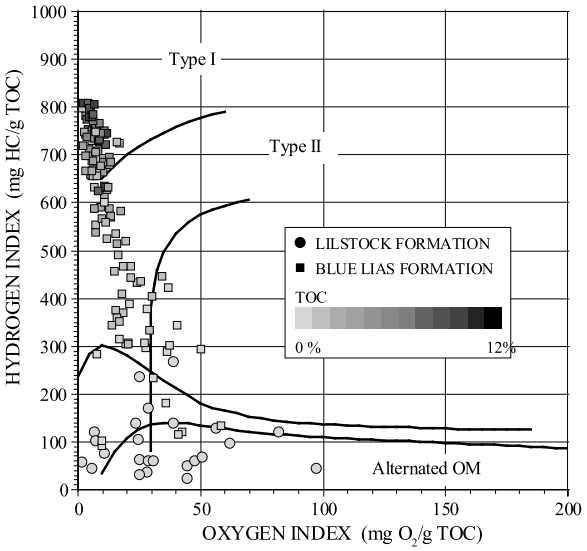

Figure 3. The Van Krevelen HI versus OI diagram drawn after RE data. Lilstock Fm samples display features of continental, altered and/or recycled OM (Type III or IV). By contrast, Blue Lias Fm samples display alternation of type II OM (marine organic matter usually constituted of spores, cuticules and animal remains) and type I OM (essentially constituted of bacteria and algae remains, i.e., picoplankton and organic-walled phytoplankton). Occurrence of type I OM is associated to exceptional sedimentary organic matter enrichment in the *planorbis* subzone (bed 7 to 24, hereafter area Z).

laminated shales, marls and limestones [*Wilson*, 1990; *Hesselbo et al.*, 2004].

3. Material and Methods

3.1. Sampling

[6] A high resolution sampling was carried out (about 8 samples per meter), starting in the Lilstock Fm and ending almost at the top of the *Planorbis* subzone of the Blue Lias Fm. The minimum duration of the *Planorbis* subzone is estimated to be 190 ka [*Weedon*, 1999] or 250 ka [*Ruhl et al.*, 2010]. The sampling is covering almost 11 m across the exposed section. The *Planorbis* subzone covers about 5 m and sampling spatial resolution is likely associated to a temporal resolution of 5–10 ka. The whole data set is reported in Figure 2.

3.2. Isotopic Analysis of Carbonates

[7] Values of $\delta^{13}C_{min}$ and $\delta^{18}O_{min}$ from carbonates were measured with a "Delta V Advantage" (ThermoScientific) isotope ratio gas mass spectrometer directly coupled to a "Kiel IV" automatic carbonate preparation device (reaction at 70°C under vacuum) at the SSMIM (Muséum National d'Histoire Naturelle of Paris, France). Analyses were calibrated via NIST 19 to the VPDB (Vienna Pee Dee Belemnite) scale. The overall precision of the measurement was better than 0.03 and 0.04‰ for carbon and oxygen isotopic composition, respectively. Reproducibility of replicated standards is typically better than +/− 0.1‰ for $\delta^{13}C_{min}$ and $\delta^{18}O_{min}$.

3.3. Isotopic Analysis of Kerogen

[8] Bulk sediments were rinsed twice with deionized water and dried before being powdered (20 to 40 g). Ten g of powdered rocks samples are processed by successive acid treatments (HCl and HF) under inert atmosphere (N_2) at 80°C followed by water washings [*Durand and Nicaise*, 1980]. Recovered kerogens are dried at 100°C under nitrogen flow, ground, weighed, and stored under inert headspace (Ar or N_2) to avoid oxidation. Nitrogen and carbon isotopic compositions on bulk sedimentary organic matter were measured on an Elemental Analyzer - Isotope Ratio Mass Spectrometer (EA-IRMS from GV Instruments). Accuracy and reproducibility were checked on laboratory organic standard ($\delta^{15}N_{org}$ = 2.1 ± 0.2 ‰ and $\delta^{13}C_{org}$ = −29.6 ± 0.2 ‰ with n = 87). This laboratory standard was calibrated for $\delta^{15}N_{org}$ values relative to international standards IAEA N1 and IAEA N2 and for $\delta^{13}C_{org}$ values relative to international standard NBS19 [*Coplen et al.*, 2006]. $\delta^{15}N_{org}$ and $\delta^{13}C_{org}$ are expressed relative to atmospheric nitrogen (AIR) and PeeDee belemnite (PDB) respectively.

3.4. Rock-Eval Analyses

[9] Analyses were performed on a Rock-Eval 6 device (IFP, France). The device was calibrated with the IFP standard 160 000, and the methodology described for bulk rocks in [*Behar et al.*, 2001] is applied. Typology of organic matter (OM) was determined using hydrogen and oxygen indexes (respectively HI and OI, reported in Figure 3, a Van-Krevelen like diagram). Tmax values, ie. temperatures at which the maximum release of hydrocarbons from cracking of kerogen occurs during pyrolysis, provide information on the thermal maturation stage of the organic matter. T_{max} values (auxiliary material) range from 412 to 430°C for the overall section attesting an excellent preservation of sedimentary organic matter.[1] Rock-Eval analyses provide both mineral carbon and sedimentary organic

[1] Auxiliary materials are available at ftp://ftp.agu.org/apend/gc/2010gc003161.

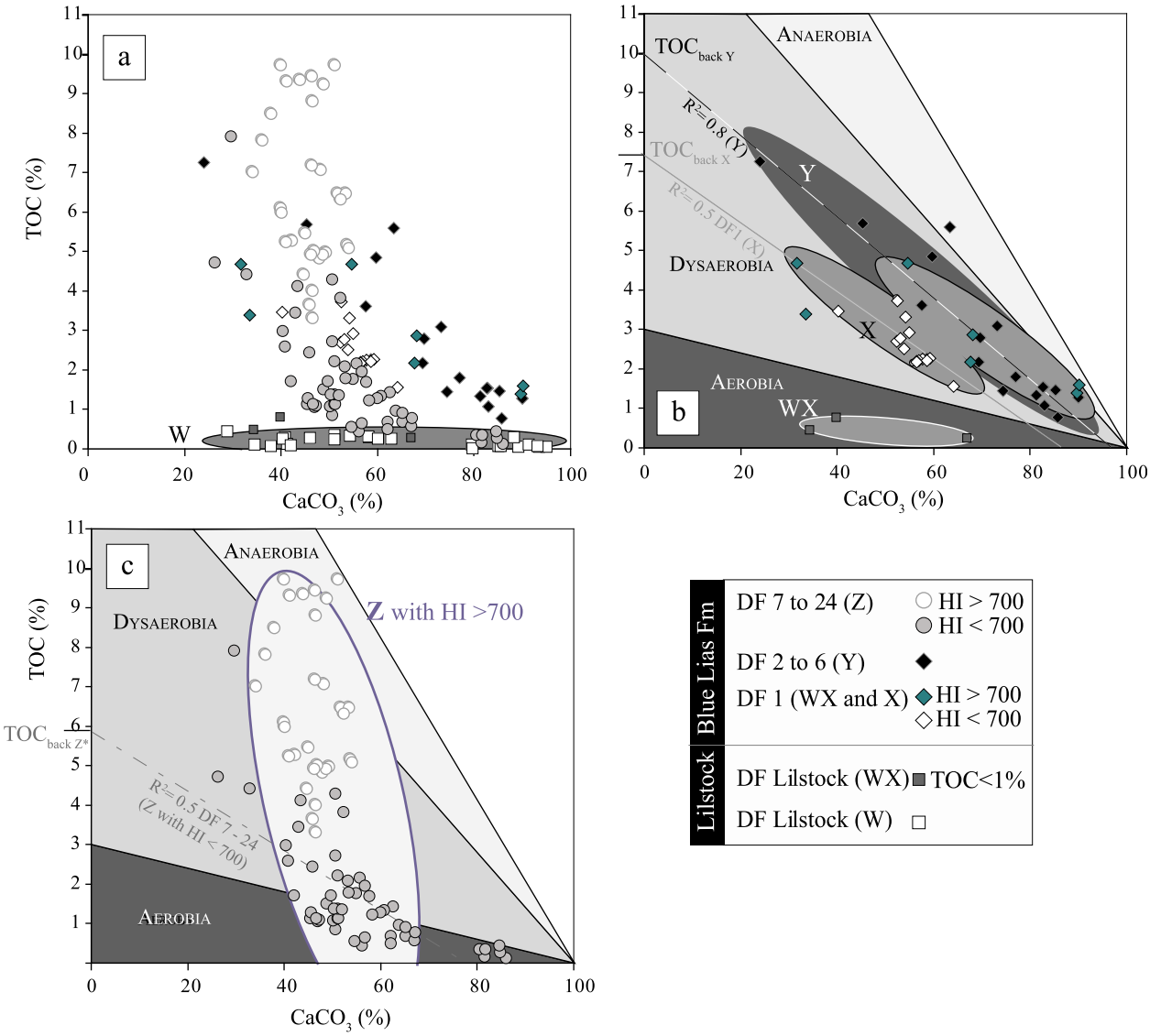

Figure 4. TOC versus $CaCO_3$ diagrams sketch in the redox conditions and the sedimentation controls of the sedimentation realm provided that sedimentation background rate and organic matter content in background component (TOC_{back}) are known [*Ricken*, 1993]. (a) Entire data set; (b) WX, W and Y domains; and (c) Z domain. A negative correlation of the TOC versus MINC crossplot indicates a sedimentation dominated by carbonates, ie. a roughly constant input of siliciclastic (SC) sediments and organic matter and variable $CaCO_3$ input. The sedimentation background rate is the SC sedimentation rate and the TOC_{back} is read as the intercept of the correlation trend with the *y* axis [*Ricken*, 1993]. As a consequence (Figure 4b), for the Blue Lias Fm bed 1, $TOC_{back\ X}$ is 7.4%. The SC sediment flux background is 20% of the total flux and the SC sedimentation rate is 4 m/My. For bed 2 to 6, $TOC_{back\ Y}$ is 10% and the SC sedimentation rate is 2m/Ma. The Z domain is dominated by OM deposition (Figure 4c) even though the samples with a HI < 700 might are deposited within a period of carbonate-dominated sedimentation as the rest of the Early Hettangian. The "aerobia, dysaerobia, anaerobia" domains reported in Figures 4b and 4c correspond to the "C I" calibration of *Ricken* [1993]. This C I case is not valid for Lilstock Formation (W domain, Figure 4a).

matter contents (respectively $CaCO_3$ weight% and TOC weight%, total organic carbon, reported in Figure 4). Quantification of two different structural components of the sedimentary organic matter is also possible during RE analyses. The first component (pyrolysable carbon, PC) can be biologically or thermally altered, roughly corresponding to aliphatic carbon chains and the second one (residual carbon, RC) can be described as a coke-like organic carbon which remains after biological and/or thermal degradation. The TOC is the sum of both components (TOC = RC+PC). Relative

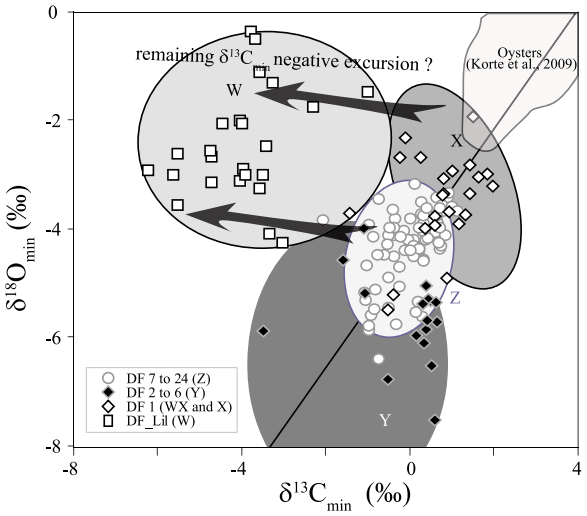

Figure 5. Crossplots of mineral oxygen and carbon isotopic compositions and of organic nitrogen and carbon isotopic compositions. The Lilstock Fm and the Blue Lias Fm samples depict two very distinct domains, suggesting strong sedimentation realm contrasts. A part of the values measured in pristine oysters by *Korte et al.* [2009] is reported.

measurement errors are below 2.5%. TOC versus $CaCO_3$ are also reported in a "Ricken diagram" [*Ricken*, 1993]. This statistically calibrated diagram depicts the sedimentation mode and the oxygenation level of the bottom waters in a three-component system: TOC, $CaCO_3$ and siliciclastic (SC) fluxes. Three different sedimentation styles are showed (Figure 4). The Lilstock Fm samples (domain W), containing mainly residual coke-like organic carbon, cannot be interpreted according to the Ricken diagram as they are deposited in a tidal environment, although they stand in the aerobic domain. Samples from pre-Planorbis beds reflect conditions of sedimentation where carbonate content fluctuate. Different domains can be defined for this part of the section according to OM fraction deposition (domains WX, X, Y). The Planorbis subzone is featured by variable deposition of OM (domain Z). Specific geochemical and environmental features of these domains will be described hereafter.

4. Definition of TJB and Correlation of $\delta^{15}N$ Record

[10] Although lateral lithological variations exist, the $\delta^{13}C_{org}$ values measured in Doniford bay kerogens describe an evolution similar in time and magnitude to the data set presented by *Hesselbo et al.* [2004] on the twin section of Saint Audrie's bay, as well as with other worldwide sections [*Guex et al.*, 2004].

[11] To define the TJB position in Doniford section, we followed the definition based on the first occurrence (FO) of *Psiloceras spelae*, the earliest Jurassic *psiloceratid* occurring at New York Canyon, USA [*Guex et al.*, 2004] and the Kuhjoch section in Austria, potential candidates for the GSSP (Global Boundary Stratotype Section and Point) of the TJB [*von Hillebrandt et al.*, 2007; *von Hillebrandt and Krystyn*, 2009]. At New York Canyon, the high-resolution ammonite biostratigraphy allowed to calibrate the $\delta^{13}C_{org}$ curve [*Guex et al.*, 2004], showing that the FO of *Psiloceras spelae* occurs within the positive CIE (Carbon Isotopic Excursion) between the two negative CIEs. *P. spelae* has not been found at Doniford. However, if we use an integrated approach that combines $\delta^{13}C_{org}$ curve shape and ammonite fauna [*Page*, 2003; *Guex et al.*, 2004], the TJB can be placed in the interval including beds 1 and 2 (Blue Lias Formation; Figure 2), where the highest values of $\delta^{13}C_{org}$ occur [*Clémence et al.*, 2010]. Using ammonite horizons, nitrogen isotope record at Doniford can be correlated with the TJ transition $\delta^{15}N_{org}$ curve from Mingolsheim core in Germany [*Quan et al.*, 2008] and from Black Bear Ridge section in British Columbia [*Sephton et al.*, 2002]. The Mingolsheim core presents a hiatus for the Planorbis subzone and starts with the *C. johnstoni* biohorizon. In Doniford, Planorbis subzone corresponds roughly to the interval from bed 2 to bed 29 [*Page*, 2005]. Absolute $\delta^{15}N$ values are higher in Doniford (from 1.5 to 5 ‰ compared to −0.5 to 2 ‰ in Mingolsheim). This offset is consistent with a strong influence of local environment on the $\delta^{15}N$ signals. At Black Bear Ridge section, after a reinterpretation of biostratigraphy first presented by *Sephton et al.* [2002], the entire Rhaetian and lowermost Jurassic appear to be extremely condensed (2.3 m of section from 61.1 to 63.4 m) if not represented by hiatus [*Hall and Pitaru*, 2003]. Thus, previous data sets are not directly comparable with those of Doniford where the early Hettangian $\delta^{15}N$ record of the Triassic-Jurassic transition is more complete.

5. Depositional Versus Diagenetical Model

[12] In the $\delta^{13}C_{min}$ versus $\delta^{18}O_{min}$ crossplot (Figure 5), Lilstock and Blue Lias Fm samples fall into two distinct clusters. A part of this bimodality is due to lower $\delta^{13}C_{min}$ values of the Lilstock samples with

respect to those of Blue Lias Fm. A second part is due to the low $\delta^{18}O_{min}$ values of the Blue Lias Fm (domain Y). This distribution is interpreted to be due to the different depositional environments and early diagenesis. The $\delta^{13}C_{min}$ and $\delta^{18}O_{min}$ signals in the Lilstock Fm are consistent with a tidal very shallow-water environment. Low $\delta^{18}O_{min}$ values are likely due to meteoric water contamination [*Brand and Veizer*, 1981]. Very low $\delta^{13}C_{min}$ values could be due to OM oxidation releasing carbon depleted in ^{13}C within the sedimentation realm. However, lower isotopic composition of $\delta^{13}C_{min}$ values is observed concomitantly to the negative $\delta^{13}C_{org}$ excursion. At Doniford, early diagenetical overprinting might have just enlarged the amplitude of carbonate excursion. The lowest $\delta^{18}O_{min}$ values in the Blue Lias Fm are found for stratigraphical beds displaying the highest $CaCO_3$ content, especially in domain Y. It is likely that, during the successive transitions from anaerobic/dysaerobic to aerobic phases, oxidized OM and sulphides produced carbonic and sulphuric acids causing carbonate dissolution and reprecipitation, as indicated by low values of $\delta^{18}O_{min}$ [*Raiswell*, 1987, 1988; *Bottrell and Raiswell*, 1989]. Such OM oxidation could also explain the locally lower $\delta^{13}C_{min}$ values (Figure 3). This agrees with a depositional-diagenetical mixed model, where lithological alternations are probably driven by primary productivity and redox cycles, and are emphasized by early diagenesis processes [*Weedon*, 1986; *Einsele et al.*, 1991].

[13] All organic matter samples display low thermal maturation indices (T_{max} < 430°C), well below the oil window, therefore excluding a significant alteration due to burial or thermal diagenesis. Despite the specific deposition realm, the $\delta^{13}C_{org}$ signal recorded at Doniford is consistent with those recorded at Saint Audrie's bay or in Austrian and German TJ sections, for Tethyan domain [*Hesselbo et al.*, 2002; *Kürschner et al.*, 2007; *van de Schootbrugge et al.*, 2008; *Ruhl et al.*, 2009], as well as with North-American T-J sections in Canada [*Ward et al.*, 2001] and Nevada [*Guex et al.*, 2004]. Furthermore, despite an isotopic signal influenced by sedimentation realm and early diagenetical conditions, the end Triassic negative $\delta^{13}C_{min}$ excursion is also observed in Italian and Hungarian sections [*Pálfy et al.*, 2001; *Galli et al.*, 2005]. Although this first $\delta^{13}C_{min}$ excursion is documented only in western Europe, this suggests an end Triassic event affecting the global carbon isotopic record. Conversely, at Doniford the early Hettangian negative excursion observed in the $\delta^{13}C_{org}$ signal is not concomitant to a clear parallel $\delta^{13}C_{min}$ excursion. The $\delta^{13}C_{min}$ bulk record show relatively high values that fluctuate around a constant average value, while obvious evidences of diagenetic alteration are not shown. This result contrasts with the $\delta^{13}C_{min}$ values measured on well-preserved oyster shells from SW Britain sections [*van de Schootbrugge et al.*, 2007; *Korte et al.*, 2009]. Their composite record parallels the early Hettangian bulk $\delta^{13}C_{org}$ negative excursion, yet with a lesser intensity.

6. Results and Interpretations

[14] Geochemical results combined with lithological and micropaleontological observations allow the definition of three distinct intervals corresponding to the Lilstock Fm, the pre-Planorbis beds and the *Planorbis* subzone. Values are reported in Data Set S1.

6.1. Upper Triassic Lilstock Fm

[15] The Lilstock Fm (W, Figure 4a) displays environmental features of tidal realm. Mudstone deposits alternate with concretionary limestones deposits and some sandy marls where ripplemarks, bioturbations and mud cracks are observed (beds L1 and L7). The $\delta^{13}C_{org}$ values record a first negative excursion (from −25.6 to −29.5 back to −26.6 ‰), almost concomitant with the highest $\delta^{15}N_{org}$ values of the section (values ranking from 3.4 to 5 ‰). According to RE analyses, the organic matter is mainly residual (RC/TOC > 0.74 with TOC lower than 0.5%) and as a consequence its origin cannot be clearly assessed. The sedimentary OM is predominantly reworked and oxidized. The range of T_{max} values indicate that this oxidation occurred by the time of deposition in subaerial environment. Such environment is not specifically documented for $\delta^{15}N$ values and the range and variations observed in the Lilstock Fm, between 3.5 ‰ and 5 ‰, is not easily interpreted. It does not appear to be consistent with a mixture of continental (lower $\delta^{15}N$ and $\delta^{13}C$) and marine (higher $\delta^{15}N$ and $\delta^{13}C$) organic matter in different proportions, deposited under aerobic conditions [*Peters et al.*, 1978]. In such shallow water tidal environment under aerobic conditions (according our RE data), diagenetical degradation of organic matter could have left the residual biomass enriched in ^{15}N. A laboratory study has directly addressed the effects of degradation on the isotopic composition of organic matter [*Lehmann et al.*, 2002]. They showed that degradation of organic matter under

aerobic conditions leaves the residual biomass enriched in ^{15}N, whereas anoxic decomposition of organic matter results in depletion of ^{15}N. In both cases, the residual biomass is depleted in ^{13}C. Tidal deposit conditions might have provided therefore altered geochemical signals that preclude further paleo-ecological interpretations. However, despite these marked local conditions, the $\delta^{13}C_{org}$ signal remains similar to the one measured in different worldwide section [*Guex et al.*, 2004].

6.2. TJ Boundary Interval, Pre-Planorbis Beds

[16] The lower part of bed 1 (WX domain) consists in a large dark gray laminated shale deposit with low carbonate content. This interval constitutes the transition from Penarth Group to Lias Group which is marked by a rapid increase of OM content, depicting an evolution from aerobia to dysaerobia (according to Ricken model, Figure 4b) and the almost total absence of microbenthos [*Clémence et al.*, 2010]. Anoxic-euxinic conditions for the "Paper Shale" at Pinhay Bay (equivalent of bed 1 at Doniford) were suggested on the basis of abundant small framboids, very low Th/U ratio and generally lack of bioturbation and benthos [*Wignall*, 2001b]. This transition occurs together with the first accumulation of type I OM observed in the section and relatively high $\delta^{13}C_{org}$ values. This level starts with the very sharp increase of $\delta^{13}C_{min}$ values at the Lilstock Fm/Blue Lias Fm transition. The sharp enrichment of well-preserved marine organic matter could outline a rapid sea level rise at this interval [*Hallam and Wignall*, 1999; *Wignall*, 2001a]. In the upper part of bed 1, the environmental conditions change (X domain). Dysaerobia dominates (Figure 4b) and type I OM is identified in most samples. In this area, two different sedimentation modes are observed in the "Ricken diagram": samples with OM characterized by HI < 700 mgHC/gTOC on the one hand and by HI > 700 on the other hand (Figure 4b). The $\delta^{13}C_{org}$ values display typical marine signatures (from −27.2 to −25.7 ‰) and $\delta^{15}N_{org}$ values slightly decrease from 3.5 to 3 ‰. The transition from upper top of bed 1 to base of bed 2 is marked by a $\delta^{15}N_{org}$ increase from 3 to 4 ‰.

[17] From bed 2 to bed 6, (Y domain), lithologies are characterized by higher $CaCO_3$ content. RE data indicate a dysaerobic environment with some anaerobic incursions (Figures 2 and 4c). As for bed 1, the type I OM is observed independently of TOC contents. Occasional lower values are observed in the $\delta^{13}C_{min}$ signal (minimal in bed 4) and during the deposition time of these beds the $\delta^{13}C_{org}$ values decrease from −25.7 to −29.6 ‰. Concomitantly to the $\delta^{13}C_{org}$ value decrease, $\delta^{15}N_{org}$ values slowly decrease from 4 to 3 ‰. The onset of this second $\delta^{13}C_{org}$ negative excursion coincides with increasing oxic level inferred from our TOC-$CaCO_3$ model and the first high abundance peak of Schizosphaerellids [*Clémence et al.*, 2010]. The next anaerobic/dysaerobic phase is concomitant with the first development of benthic foraminifera (Figure 2).

6.3. Lowermost Jurassic Blue Lias Formation Planorbis Subzone

[18] This zone (Z) corresponds to the second carbon isotope negative anomaly (or "main excursion" according to *Hesselbo et al.* [2002]) following the T/J boundary and the sedimentation realm is described as outer-shelf marine water [*Hesselbo et al.*, 2004]. The alternation of limestone, mudstone, and shale deposition is observed together with a parallel alternation of aerobic, dysaerobic and anaerobic conditions defined after Rock-Eval data in the "Ricken diagram."

[19] A short wave rhythmic pattern is established for all measured geochemical signals (Figure 2). Both $\delta^{13}C_{org}$ and $\delta^{15}N_{org}$ values fluctuate in a 2‰ range, respectively from −30 to −28 ‰, and from 1.7 to 3.2 ‰. $\delta^{13}C_{org}$ and $\delta^{15}N_{org}$ values are relatively higher as aerobic to dysaerobic conditions occur while TOC content and HI are lower, i.e., type II OM is produced when more oxygenated conditions exists in the water column. Type I OM occurs only when TOC contents are higher than 3.5% and is characterized by lower $\delta^{13}C_{org}$ and $\delta^{15}N_{org}$ values when dysaerobic to anaerobic conditions are depicted in the "Ricken diagram." The RE-defined dysaerobic-aerobic conditions are consistent with dysoxic events defined from micropaleontological data [*Clémence et al.*, 2010]. Abundance peaks of calcareous phytoplankton and development of opportunist calcareous benthic foraminifers, combined with decrease of OM might indicate dysoxic phases and transient recovery of the carbonate biological pump. Anoxic conditions are highlighted by absence of benthic foraminifers together with higher contents in OM. It is possible to draw a comparison between our data and the early Jurassic succession (Blue Lias Fm) of organic-walled phytoplankton in Saint Audrie's bay [*van de Schootbrugge et al.*, 2007] for the early Jurassic (Figure 2) based on $\delta^{13}C_{org}$ stratigraphy. However, the correlation is not trivial because of lateral variations of the beds between

the two sections. There is a clear alternation of aerobic and anaerobic/dysaerobic conditions in the water column reflected by calcareous and organic-walled microorganisms alternation in the Bristol Channel Basin at the base of the early Hettangian [*van de Schootbrugge et al.*, 2007; *Clémence et al.*, 2010]. In interval Y, a high abundance peak of organic-walled dinoflagellate cysts occurs during anaerobic conditions. In domain Z, the comparison between both sections reveal that anaerobic and dysaerobic conditions are characterized by higher values of TOC and HI together with abundance peaks of prasinophytes and organic-walled dinocysts.

7. Aftermath in the Bristol Channel Basin

7.1. Interpretation of the $\delta^{15}N_{org}$ Signal

[20] Sedimentological, paleontolongical and geochemical data depict variations in redox conditions for sedimentation realm during deposition time of the Blue Lias Fm. Short-lasting $\delta^{15}N_{org}$ decreases are observed during anaerobic phases, as type I OM exceptional accumulations occur.

[21] In modern environments, the $\delta^{15}N_{org}$ values are controlled by nitrate concentration, availability and isotopic composition in seawater. Modern $\delta^{15}N$ average signature of deep nitrates is ca. +6 ‰ and sinking organic matter below well ventilated surface waters roughly records this isotopic composition [*Thunell et al.*, 2004]. Variations of this isotopic average value depend on redox conditions and reported modern values in organic matter mainly range from −2 to +10 ‰ [*Wada et al.*, 1975; *Peters et al.*, 1978; *Wada and Hattori*, 1978; *Altabet*, 1996; *Thunell and Kepple*, 2004]. The $\delta^{15}N_{org}$ values recorded in the Z domain, ranging from 1.7 to 3.2 ‰, are low compared to average modern values. There is no constrains on the average $\delta^{15}N$ of deep nitrates in the Bristol Chanel basin at that time. However, the low $\delta^{15}N_{org}$ values suggest that this average value is lower than the modern one. There is no evidence that the average $\delta^{15}N$ of the global ocean deep nitrates significantly evolved during Phanerozoic times at equivalent global redox conditions [*Beaumont and Robert*, 1999], thus suggesting a relative isolation of the Bristol Chanel basin. The 1.5 ‰ shortwave variations can be interpreted as reflecting seawater column oxygen level variations because of (1) low availability of dissolved nitrates and switch from nitrate assimilation to diazotrophy followed by ammonium assimilation during primary production (2) high availability of dissolved nitrates, and/or (3) organic matter degradation.

[22] Regarding hypothesis (1), in recent sediments, conditions of suboxic subsurface water environments are reflected by ^{15}N enrichments of the organic matter, induced by denitrification that enriches the nitrate pool in ^{15}N and decreases its availability [*Altabet et al.*, 1995; *Ganeshram et al.*, 1995; *Ganeshram et al.*, 2002]. No such ^{15}N enrichments are observed in the Bristol Channel Basin concomitantly with anaerobic events based on RE data. On the opposite, these events are associated with a decrease of $\delta^{15}N_{org}$ values. If hypoxic conditions are envisioned, the nitrate pool is entirely used and another source of inorganic nitrogen, namely atmospheric N_2 or ammonium, is required to fuel primary production in the basin. In the modern ocean, nitrogen fixation is promoted in the absence of other inorganic nitrogen source because of the high energetic cost of N_2 fixation [*Fay*, 1992]. N_2-fixer organisms are prokaryotes including cyanobacteria, purple and green bacteria. They characterize environments poor in nutrient or with strong redox gradients, mainly in O_2-poor environments [*Berman-Frank et al.*, 2003]. The switch from nitrate assimilation to N_2-fixation has been highlighted in different Cretaceous oceanic anoxic event (OAE) records, for which negative excursions of $\delta^{15}N_{org}$ values are reported [*Rau et al.*, 1987; *Jenkyns et al.*, 2002; *Dumitrescu and Brassell*, 2006; *Meyers*, 2006; *Meyers et al.*, 2009]. Using biomarkers to investigate the nature of organic matter deposited during early Aptian OAE-1a and late Cenomanian OAE-2 of the middle Cretaceous, *Kuypers et al.* [2004] give evidence that nitrogen-fixers are the main primary producers. N_2 fixation leads to nitrogen isotopic composition in organic matter closer to that of atmospheric nitrogen for which $\delta^{15}N$ = 0 ‰ [*Wada et al.*, 1975; *Minagawa and Wada*, 1986; *Beaumont et al.*, 2000]. In the Bristol Channel Basin, the accumulation of type I OM supports the "blooming" of prokaryotic organic-walled organisms as main primary producers. Additionally to N_2-fixation, the occurrence of lower $\delta^{15}N_{org}$ values could be explained by the use of ammonium as inorganic nitrogen supplier for non N_2-fixers organisms, as ammonium assimilation may lead to ^{14}N enriched organic matter relative to source [*Beaumont et al.*, 2000]. However, this first hypothesis appears to be hardly reconciled with the recorded $\delta^{15}N_{org}$ value range that

remains clearly higher than atmospheric N_2 isotopic composition.

[23] Alternatively, this OM accumulation could be interpreted as (2) the settling of eutrophic conditions due to the increase of nutrient inputs within the basin. *Calvert et al.* [1992] documented $\delta^{15}N_{org}$ values in the 0 to 4 ‰ range associated with relatively low $\delta^{13}C_{org}$ values during formation of sapropel horizons in the eastern Mediterranean. This range of values has been interpreted as reflecting enhanced productivity during eutrophic conditions associated with high dissolved inorganic nitrogen (nitrate and/or ammonia) contents [*Wada and Hattori*, 1978; *Calvert et al.*, 1992]. Eutrophic conditions promote organic-walled organism "blooming" in modern environments. During the early Hettangian recovery (Z), while organic-walled organism high abundance peaks occur, higher organic productivity is depicted according to "Ricken diagram" (Figures 2 and 4). These high abundances are likely to "poison" surface waters and to generate a large export of organic matter. This export generates anaerobic/dysaerobic conditions in bottom waters and spectacular type I OM accumulation.

[24] In the third case (3), the $\delta^{15}N_{org}$ signal would be the result of organic matter degradation during the exportation through seawater column. Aerobic waters could tend to promote organic matter oxidation and to increase $\delta^{15}N_{org}$ values of the sinking OM [*Sachs and Repeta*, 1999]. However, this interpretation has been challenged since [*Higgins et al.*, 2010]. Higgins *et al.* showed that the $\delta^{15}N_{org}$ variations are not due to OM alteration and that sedimentary OM faithfully records the seawater nitrate $\delta^{15}N$ in coastal settings [*Altabet et al.*, 1999; *Thunell and Kepple*, 2004].

[25] According to these three hypotheses, the signal reveals the different conditions of water column oxygenation. The higher $\delta^{15}N_{org}$ values then reflect higher oxygen content in the seawater column which is consistent with the lower TOC measured in the sediments and the lower $\delta^{13}C_{min}$ values that could reflect this organic matter degradation. These phases correspond to periods of more ventilated water column and more efficient recycling of nutrients, favoring calcareous phytoplankton surface production (high abundance peaks of Schizosphaerellids) generally coupled with the development of calcareous benthic fauna [*Clémence et al.*, 2010]. However, these benthic foraminifer assemblages are characterized by a very low diversity and are dominated by opportunist species tolerant with low oxygen conditions, witnessing stressful conditions in bottom waters.

7.2. Scenarios

[26] Two scenarios are likely. The first one, or hypothesis (1), consists in invoking periods of stagnant waters leading to a lower recycling of nutrients within the seawater column, generating oligotrophic conditions at the surface. This leads to development of N_2-fixers and accumulation of OM at the seafloor. These events occur in alternation with aerobic/dysaerobic conditions linked to a better ventilation of seawater column. Abundance peaks of calcareous phytoplankton coupled with development of opportunist calcareous benthic foraminifers represented transient phases of reventilation of column water and of carbonate pump recovery. The second scenario or hypothesis (2) consists in suggesting an orbital control of climate leading to variations of continental runoff that delivers more nutrients to the photic zone of the epicontinental basin of Doniford. This increase in nutrient input allows a higher production that leads to a more important OM export, leading to anaerobic conditions of bottom waters and OM accumulation. The investigation of Early Bajocian calcareous production crisis shows that this increase in primary production could inhibit calcareous production [*Paris et al.*, 2010]. Calcareous phytoplankton communities are thus disfavored. During times of lower runoff, surface production and OM accumulation decrease. The decrease of eutrophic conditions in the basin and re-oxygenation of bottom waters allow the establishment of benthic and pelagic calcareous communities. However, environmental conditions remain stressful as indicated by the low diversity of micropaleontological assemblages [*Clémence et al.*, 2010]. In conclusion, OM accumulation events are associated with stressed bottom water conditions and no calcareous surface productivity while periods of lower OM accumulation reflect relatively elaborated food webs including calcareous phytoplankton and microbenthos [*Clémence et al.*, 2010]. The exact cause of these oscillations is not clear. The marly limestone alternations of the Blue Lias Fm. have been interpreted has reflecting Milankovitch cycles [*Weedon*, 1999]. This oscillating trend indicates that environmental recovery is not achieved and that ecosystems are not robust and very sensitive to any external perturbation. To discriminate between scenarios 1 and 2, further proxies are needed, as for example the sedimentary [Mo], to better understand the degree of restriction and temporal changes of deep-water renewal of the basin [*Algeo and Lyons*,

2006] and biomarkers to ensure the potential occurrence of N_2-fixers.

8. Conclusion

[27] This study provides new information on the end Triassic crisis aftermath. In the Bristol Channel Basin, at Doniford, the organic matter of Lilstock Formation was deeply altered because of deposition in subaerial tidal conditions during a sealevel lowstand. The only clue of the global crisis is the negative isotopic composition of $\delta^{13}C_{org}$ values and, likely, that of $\delta^{13}C_{min}$ values which have been reported for deeper environments. We cannot exclude that, at Doniford, due to very tidal shallow environment conditions of Lilstock Formation, the high input of continental organic matter and its recycling have amplified both $\delta^{13}C_{org}$ and $\delta^{13}C_{min}$ negative signal during the late Rhaetian.

[28] The aftermath is characterized by a three-step environmental recovery during sea level rise. The first step is described as a period of dysaerobic/anaerobic conditions and less negative $\delta^{13}C_{org}$ values. Accumulation of type I OM is observed (3–5%) probably issued from organic-walled phytoplankton. The second step is marked by the first exceptional accumulation of type I OM (>7%) with the onset of the second $\delta^{13}C_{org}$ negative excursion. The third step is characterized by a succession of type I OM accumulation with relatively lower $\delta^{15}N_{org}$ values. These OM accumulations are probably due to high abundances of organic-walled prokaryotic organisms generating dysaerobic/anaerobic conditions in bottom waters. The different groups of organisms, organic-walled phytoplankton, calcareous nannoplankton and foraminifera are affected by the environmental oscillations during the "recovery" phase in the early Jurassic. Ecosystems developing during the early Hettangian recovery phase are not robust and be very sensitive to any climatic variations such as induced by Milankovitch cycles, indicating an environment that remain perturbed after the end Triassic mass extinction.

Acknowledgments

[29] We are very grateful to Jean Guex for precious discussions. We thank Ramon Martinez (IFP) for kerogen extraction. This work was granted through IFP-IPGP convention 31–231. This is IPGP contribution 3037.

References

Algeo, T. J., and T. W. Lyons (2006), Mo-total organic carbon covariation in modern anoxic marine environments: Implications for analysis of paleoredox and paleohydrographic conditions, *Paleoceanography*, *21*, PA1016, doi:10.1029/2004PA001112.

Altabet, M. A. (1996), Nitrogen and carbon isotopic traceurs of the source and transformation of particles in the deep sea, in *Particle Flux in the Ocean*, edited by V. Ittekkot et al., pp. 155–184, John Wiley, Chichester.

Altabet, M. A., R. Francois, D. W. Murray, and W. L. Prell (1995), Climate-related variations in denitrification in the Arabian Sea from sediment $^{15}N/^{14}N$ ratios, *Nature*, *373*, 506–509, doi:10.1038/373506a0.

Altabet, M. A., C. Pilskaln, R. Thunell, C. Pride, D. Sigman, F. Chavez, and R. Francois (1999), The nitrogen isotope biogeochemistry of sinking particles from the margin of the eastern North Pacific, *Deep Sea Res., Part I*, *46*(4), 655–679, doi:10.1016/S0967-0637(98)00084-3.

Barras, C. G., and R. J. Twitchett (2007), Response of the marine infauna to Triassic-Jurassic environmental change: Ichnological data from southern England, *Palaeogeogr. Palaeoclimatol. Palaeoecol.*, *244*, 223–241, doi:10.1016/j.palaeo.2006.06.040.

Beaumont, V., and F. Robert (1999), Nitrogen isotope ratios of kerogens in Precambrian cherts: A record of the evolution of atmosphere chemistry?, *Precambrian Res.*, *96*, 63–82, doi:10.1016/S0301-9268(99)00005-4.

Beaumont, V., L. L. Jahnke, and D. J. Des Marais (2000), Nitrogen isotopic fractionation in the synthesis of photosynthetic pigments, in *Rhodobacter capsulatus* and *Anabaena cylindrica*, *Org. Geochem.*, 31, 1075–1085, doi:10.1016/S0146-6380(00)00133-9.

Beerling, D. J., and R. A. Berner (2002), Biogeochemical constraints on the Triassic-Jurassic boundary carbon cycle event, *Global Biogeochem. Cycles*, *16*(3), 1036, doi:10.1029/2001GB001637.

Behar, F., V. Beaumont, H. L. De, and B. Penteado (2001), Rock-Eval 6 technology: Performances and developments, *Oil Gas Sci. Technol.*, *56*(2), 111–134.

Berman-Frank, I., P. Lundgren, and P. Falkowski (2003), Nitrogen fixation and photosynthetic oxygen evolution in cyanobacteria, *Res. Microbiol.*, *154*(3), 157–164, doi:10.1016/S0923-2508(03)00029-9.

Bottrell, S., and R. Raiswell (1989), Primary versus diagenetic origin of Blue Lias rhythms (Dorset, UK): Evidence from sulphur geochemistry, *Terra Nova*, *1*(5), 451–456, doi:10.1111/j.1365-3121.1989.tb00409.x.

Brand, U., and J. Veizer (1981), Chemical diagenesis of a multicomponent system—II. Stable isotopes, *J. Sediment. Petrol.*, *51*, 987–998.

Calvert, S. E., B. Nielsen, and M. R. Fontugne (1992), Evidence from nitrogen isotope ratios for enhanced productivity during formation of eastern Mediterranean sapropels, *Nature*, *359*, 223–225, doi:10.1038/359223a0.

Cirilli, S., A. Marzoli, L. Tanner, H. Bertrand, N. Buratti, F. Jourdan, G. Bellieni, D. Kontak, and P. R. Renne (2009), Latest Triassic onset of the Central Atlantic Magmatic Province (CAMP) volcanism in the Fundy Basin (Nova Scotia): New stratigraphic constraints, *Earth Planet. Sci. Lett.*, *286*(3–4), 514–525, doi:10.1016/j.epsl.2009.07.021.

Clémence, M.-E., A. Bartolini, S. Gardin, G. Paris, V. Beaumont, and K. N. Page (2010), Early Hettangian benthic-planktonic

coupling at Doniford (SW England): Palaeoenvironmental implications for the aftermath of the end-Triassic crisis, *Palaeogeogr. Palaeoclimatol. Palaeoecol.*, doi:10.1016/j.palaeo.2010.05.021, in press.

Coplen, T. B., W. A. Brand, M. Gehre, M. Groning, H. A. J. Meijer, B. Toman, and R. M. Verkouteren (2006), New guidelines for $\delta^{13}C$ measurements, *Anal. Chem.*, *78*(7), 2439–2441, doi:10.1021/ac052027c.

Courtillot, V. (1994), Mass extinctions in the last 300 million years: One impact and seven flood basalts?, *Isr. J. Earth Sci.*, *43*, 255–266.

Dumitrescu, M., and S. C. Brassell (2006), Compositional and isotopic characteristics of organic matter for the early Aptian Oceanic Anoxic Event at Shatsky Rise, ODP Leg 198, *Palaeogeogr. Palaeoclimatol. Palaeoecol.*, *235*(1–3), 168–191, doi:10.1016/j.palaeo.2005.09.028.

Durand, B., and G. Nicaise (1980), Procedures for kerogen isolation, in *Kerogen-Insoluble Organic Matter From Sedimentary Rocks*, edited by B. Durand, pp. 35–53, Technip, Paris.

Einsele, G., W. Ricken, A. Seilacher, G. Einsele, W. Ricken, and A. Seilacher (1991), *Cycles and Events in Stratigraphy*, Springer, New York.

Fay, P. (1992), Oxygen relations of nitrogen fixation in cyanobacteria, *Microbiol. Rev.*, *56*(2), 340–373.

Galli, M. T., F. Jadoul, S. M. Bernasconi, and H. Weissert (2005), Anomalies in global carbon cycling and extinction at the Triassic/Jurassic boundary: Evidence from a marine C-isotope record, *Palaeogeogr. Palaeoclimatol. Palaeoecol.*, *216*(3–4), 203–214, doi:10.1016/j.palaeo.2004.11.009.

Ganeshram, R. S., T. F. Pedersen, S. E. Calvert, and J. W. Murray (1995), Large changes in oceanic nutrient inventories from glacial to interglacial periods, *Nature*, *376*, 755–758, doi:10.1038/376755a0.

Ganeshram, R. S., T. F. Pedersen, S. Calvert, and R. François (2002), Reduced nitrogen fixation in the glacial ocean inferred from changes in marine nitrogen and phosphorus inventories, *Nature*, *415*(6868), 156–159, doi:10.1038/415156a.

Guex, J., A. Bartolini, V. Atudorei, and D. Taylor (2004), High-resolution ammonite and carbon isotope stratigraphy across the Triassic-Jurassic boundary at New York Canyon (Nevada), *Earth Planet. Sci. Lett.*, *225*(1–2), 29–41, doi:10.1016/j.epsl.2004.06.006.

Hall, R. L., and S. Pitaru (2003), Carbon and nitrogen isotope disturbances and an end-Norian (Late Triassic) extinction event: Comment and reply, *Geology*, *31*(6), e24–e25, doi:10.1130/0091-7613(2003)31<e24:CANIDA>2.0.CO;2.

Hallam, A. (1992), *Phanerozoic Sea-Level Changes*, Columbia Univ. Press, New York.

Hallam, A., and P. B. Wignall (1999), Mass extinctions and sea-level changes, *Earth Sci. Rev.*, *48*(4), 217–250, doi:10.1016/S0012-8252(99)00055-0.

Hesselbo, S., S. Robinson, F. Surlyk, and S. Piasecki (2002), Terrestrial and marine extinction at the Triassic-Jurassic boundary synchronized with major carbon-cycle perturbation: A link to initiation of massive volcanism?, *Geology*, *30*(3), 251–254, doi:10.1130/0091-7613(2002)030<0251:TAMEAT>2.0.CO;2.

Hesselbo, S., S. Robinson, and F. Surlyk (2004), Sea-level change and facies development across potential Triassic-Jurassic boundary horizons, SW Britain, *J. Geol. Soc.*, *161*(3), 365–379.

Hesselbo, S. P., C. A. McRoberts, and J. Pálfy (2007), Triassic-Jurassic boundary events: Problems, progress, possibilities, *Palaeogeogr. Palaeoclimatol. Palaeoecol.*, *244*(1–4), 1–10, doi:10.1016/j.palaeo.2006.06.020.

Higgins, M. B., R. S. Robinson, S. J. Carter, and A. Pearson (2010), Evidence from chlorin nitrogen isotopes for alternating nutrient regimes in the eastern Mediterranean Sea, *Earth Planet. Sci. Lett.*, *290*(1–2), 102–107, doi:10.1016/j.epsl.2009.12.009.

Hounslow, M. W., P. E. Posen, and G. Warrington (2004), Magnetostratigraphy and biostratigraphy of the Upper Triassic and lowermost Jurassic succession, St. Audrie's Bay, UK, *Palaeogeogr. Palaeoclimatol. Palaeoecol.*, *213*(3–4), 331–358, doi:10.1016/j.palaeo.2004.07.018.

Jenkyns, H. C., C. E. Jones, D. R. Gröcke, and S. P. Hesselbo (2002), Chemostratigraphy of the Jurassic System: Applications, limitations and implications for palaeoceanography, *J. Geol. Soc.*, *159*, 351–378, doi:10.1144/0016-764901-130.

Knight, K. B., S. Nomade, P. R. Renne, A. Marzoli, H. Bertrand, and N. Youbi (2004), The Central Atlantic Magmatic Province at the Triassic-Jurassic boundary: Paleomagnetic and $^{40}Ar/^{39}Ar$ evidence from Morocco for brief, episodic volcanism, *Earth Planet. Sci. Lett.*, *228*(1–2), 143–160, doi:10.1016/j.epsl.2004.09.022.

Korte, C., S. P. Hesselbo, H. C. Jenkyns, R. E. M. Rickaby, and C. Spotl (2009), Palaeoenvironmental significance of carbon-and oxygen-isotope stratigraphy of marine Triassic-Jurassic boundary sections in SW Britain, *J. Geol. Soc.*, *166*(3), 431, doi:10.1144/0016-76492007-177.

Kürschner, W. M., N. R. Bonis, and L. Krystyn (2007), Carbon-isotope stratigraphy and palynostratigraphy of the Triassic-Jurassic transition in the Tiefengraben section-Northern Calcareous Alps (Austria), *Palaeogeogr. Palaeoclimatol. Palaeoecol.*, *244*(1–4), 257–280, doi:10.1016/j.palaeo.2006.06.031.

Kuypers, M. M. M., Y. Van Breugel, S. Schouten, E. Erba, and J. S. S. Damsté (2004), N_2-fixing cyanobacteria supplied nutrient N for Cretaceous oceanic anoxic events, *Geology*, *32*(10), 853–856, doi:10.1130/G20458.1.

Lehmann, M. F., S. M. Bernasconi, A. Barbieri, and J. A. McKenzie (2002), Preservation of organic matter and alteration of its carbon and nitrogen isotope composition during simulated and in situ early sedimentary diagenesis, *Geochim. Cosmochim. Acta*, *66*(20), 3573–3584, doi:10.1016/S0016-7037(02)00968-7.

Mander, L., R. J. Twitchett, and M. J. Benton (2008), Palaeoecology of the Late Triassic extinction event in the SW UK, *J. Geol. Soc.*, *165*, 319–332, doi:10.1144/0016-76492007-029.

Marzoli, A., H. Bertrand, K. Knight, S. Cirilli, N. Buratti, C. Verati, S. Nomade, P. Renne, N. Youbi, and R. Martini (2004), Synchrony of the Central Atlantic magmatic province and the Triassic-Jurassic boundary climatic and biotic crisis, *Geology*, *32*(11), 973–976, doi:10.1130/G20652.1.

McHone, J. G. (2002), Volatile emissions from Central Atlantic Magmatic Province basalts: Mass assumptions and environmental consequences, in *The Central Atlantic Magmatic Province: Insights From Fragments of Pangea*, *Geophys. Monogr. Ser.*, vol. 136, edited by W. Hames et al., pp. 241–254, AGU, Washington, D. C.

Meyers, P. A. (2006), Paleoceanographic and paleoclimatic similarities between Mediterranean sapropels and Cretaceous black shales, *Palaeogeogr. Palaeoclimatol. Palaeoecol.*, *235*(1–3), 305–320, doi:10.1016/j.palaeo.2005.10.025.

Meyers, P. A., S. M. Bernasconi, and J. G. Yum (2009), 20 My of nitrogen fixation during deposition of mid-Cretaceous black shales on the Demerara Rise, equatorial Atlantic

Ocean, *Org. Geochem.*, *40*(2), 158–166, doi:10.1016/j.orggeochem.2008.11.006.

Minagawa, M., and E. Wada (1986), Nitrogen isotope ratios of red tide organisms in the East China Sea: A characterization of biological nitrogen fixation, *Mar. Chem.*, *19*(3), 245–259, doi:10.1016/0304-4203(86)90026-5.

Nomade, S., K. Knight, E. Beutel, P. Renne, C. Verati, G. Féraud, A. Marzoli, N. Youbi, and H. Bertrand (2007), Chronology of the Central Atlantic Magmatic Province: Implications for the Central Atlantic rifting processes and the Triassic-Jurassic biotic crisis, *Palaeogeogr. Palaeoclimatol. Palaeoecol.*, *244*(1–4), 326–344, doi:10.1016/j.palaeo.2006.06.034.

Page, K. N. (2003), The Lower Jurassic of Europe—Its subdivision and correlation, in *The Jurassic of Denmark and Greenland*, *Bull. 1*, edited by J. R. Ineson and F. Surlyk, pp. 23–60, Geol. Surv. of Den. and Greenl., Copenhagen.

Page, K. N. (2005), The Hettangian ammonite faunas of the West Somerset coast (south west England) and their significance for the correlation of the candidate GSSP (Global Stratotype and Point) for the base of the Jurassic System at St. Audries Bay, paper presented at Colloque Hettangien à Hettange, de la science au patrimoine, Univ. Henri Poncaré, Hettange-Grande, France, 1–3 April.

Pálfy, J., A. Demeny, J. Haas, M. Hetenyi, M. Orchard, and I. Veto (2001), Carbon isotope anomaly and other geochemical changes at the Triassic-Jurassic boundary from a marine section in Hungary, *Geology*, *29*(11), 1047–1050, doi:10.1130/0091−7613(2001)029<1047:CIAAOG>2.0.CO;2.

Pálfy, J., et al. (2007), Triassic−Jurassic boundary events inferred from integrated stratigraphy of the Csovar section, Hungary, Palaeogeogr. *Palaeoclimatol. Palaeoecol.*, *244*(1–4), 11–33, doi:10.1016/j.palaeo.2006.06.021.

Paris, G., A. Bartolini, Y. Donnadieu, V. Beaumont, and J. Gaillardet (2010), Investigating boron isotopes in a middle Jurassic limestone sequence, *Chem. Geol.*, doi:10.1016/j.chemgeo.2010.03.013, in press.

Peters, K. E., R. E. Sweeney, and I. R. Kaplan (1978), Correlation of carbon and nitrogen stable isotope ratios in sedimentary organic matter, *Limnol. Oceanogr.*, *23*(4), 598–604, doi:10.4319/lo.1978.23.4.0598.

Quan, T. M., B. van de Schootbrugge, M. P. Field, Y. Rosenthal, and P. G. Falkowski (2008), Nitrogen isotope and trace metal analyses from the Mingolsheim core (Germany): Evidence for redox variations across the Triassic-Jurassic boundary, *Global Biogeochem. Cycles*, *22*, GB2014, doi:10.1029/2007GB002981.

Raiswell, R. (1987), Non-steady state microbiological diagenesis and the origin of concretions and nodular limestones, *Geol. Soc. London Spec. Publ.*, *36*(1), 41–54, doi:10.1144/GSL.SP.1987.036.01.05.

Raiswell, R. (1988), Chemical model for the origin of minor limestone-shale cycles by anaerobic methane oxidation, *Geology*, *16*(7), 641, doi:10.1130/0091-7613(1988)016<0641:CMFTOO>2.3.CO;2.

Rau, G. H., M. A. Arthur, and W. E. Dean (1987), $^{15}N/^{14}N$ variations in Cretaceous Atlantic sedimentary sequences: Implication for past changes in marine nitrogen biogeochemistry, *Earth Planet. Sci. Lett.*, *82*(3–4), 269–279, doi:10.1016/0012-821X(87)90201-9.

Raup, D. M., and J. J. Sepkoski (1982), Mass extinctions in the marine fossil record, *Science*, *215*(4539), 1501, doi:10.1126/science.215.4539.1501.

Ricken, W. (1993), *Sedimentation as a Three-Component System*, Springer, Berlin.

Ruhl, M., W. M. Kürschner, and L. Krystyn (2009), Triassic-Jurassic organic carbon isotope stratigraphy of key sections in the western Tethys realm (Austria), *Earth Planet. Sci. Lett.*, *281*(3–4), 169–187, doi:10.1016/j.epsl.2009.02.020.

Ruhl, M., M. H. L. Deenen, H. A. Abels, N. R. Bonis, W. Krijgsman, and W. M. Kürschner (2010), Astronomical constraints on the duration of the early Jurassic Hettangian stage and recovery rates following the end-Triassic mass extinction (St Audrie's Bay/East Quantoxhead, UK), *Earth Planet. Sci. Lett.*, *295*(1–2), 262–276, doi:10.1016/j.epsl.2010.04.008.

Sachs, J. P., and D. J. Repeta (1999), Oligotrophy and nitrogen fixation during eastern Mediterranean sapropel events, *Science*, *286*(5449), 2485, doi:10.1126/science.286.5449.2485.

Schoene, B., J. Guex, A. Bartolini, U. Schaltegger, and T. J. Blackburn (2010), Correlating the end-Triassic mass extinction and flood basalt volcanism at the 100 ka level, *Geology*, *38*(5), 387–390, doi:10.1130/G30683.1.

Sephton, M. A., K. Amor, I. A. Franchi, P. B. Wignall, R. Newton, and J. P. Zonneveld (2002), Carbon and nitrogen isotope disturbances and an end-Norian (Late Triassic) extinction event, *Geology*, *30*(12), 1119–1122, doi:10.1130/0091-7613(2002)030<1119:CANIDA>2.0.CO;2.

Thunell, R. C., and A. B. Kepple (2004), Glacial-Holocene $\delta^{15}N$ record from the Gulf of Tehuantepec, Mexico: Implications for denitrification in the eastern equatorial Pacific and changes in atmospheric N_2O, *Global Biogeochem. Cycles*, *18*(1), GB1001, doi:10.1029/2002GB002028.

Thunell, R. C., D. M. Sigman, F. Muller-Karger, Y. Astor, and R. Varela (2004), Nitrogen isotope dynamics of the Cariaco Basin, Venezuela, *Global Biogeochem. Cycles*, *18*, GB3001, doi:10.1029/2003GB002185.

Tomašových, A., and M. Siblik (2007), Evaluating compositional turnover of brachiopod communities during the end-Triassic mass extinction (Northern Calcareous Alps): Removal of dominant groups, recovery and community reassembly, *Palaeogeogr. Palaeoclimatol. Palaeoecol.*, *244*(1–4), 170–200, doi:10.1016/j.palaeo.2006.06.028.

Twitchett, R. J., and C. G. Barras (2004), Trace fossils in the aftermath of mass extinction events, in *The Application of Ichnology to Palaeoenvironmental and Stratigraphic Analysis*, edited by D. McIlroy, pp. 397–418, Geol. Soc., London.

van de Schootbrugge, B., F. Tremolada, Y. Rosenthal, T. R. Bailey, S. Feist-Burkhardt, H. Brinkhuis, J. Pross, D. V. Kent, and P. G. Falkowski (2007), End-Triassic calcification crisis and blooms of organic-walled 'disaster species,' *Palaeogeogr. Palaeoclimatol. Palaeoecol.*, *244*(1–4), 126–141, doi:10.1016/j.palaeo.2006.06.026.

van de Schootbrugge, B., J. L. Payne, A. Tomasovych, J. Pross, J. Fiebig, M. Benbrahim, K. B. Föllmi, and T. M. Quan (2008), Carbon cycle perturbation and stabilization in the wake of the Triassic-Jurassic boundary mass-extinction event, *Geochem. Geophys. Geosyst.*, *9*, Q04028, doi:10.1029/2007GC001914.

van de Schootbrugge, B., T. M. Quan, S. Lindström, W. Püttmann, C. Heunisch, J. Pross, J. Fiebig, R. Petschick, H. G. Röhling, and S. Richoz (2009), Floral changes across the Triassic/Jurassic boundary linked to flood basalt volcanism, *Nat. Geosci.*, *2*, 589–594, doi:10.1038/ngeo577.

von Hillebrandt, A., and L. Krystyn (2009), On the oldest Jurassic ammonites of Europe (Northern Calcareous Alps, Austria) and their global significance, *Neues Jahrb. Geol. Palaeontol. Abh.*, *253*(2–3), 163–195, doi:10.1127/0077-7749/2009/0253-0163.

von Hillebrandt, A., L. Krystyn, W. M. Kürschner, P. R. Bown, C. McRoberts, M. Ruhl, M. Simms, A. Tomasovych, and M. Urlichs (2007), A candidate GSSP for the base of the Jurassic in the Northern Calcareous Alps (Kuhjoch section, Karwendel Mountains, Tyrol, Austria, *ISJS Newsl.*, *24*(1), 2–20.

Wada, E., and A. Hattori (1978), Nitrogen isotope effects in the assimilation of inorganic nitrogenous compounds by marine diatoms, *Geomicrobiol. J.*, *1*(1), 85–101, doi:10.1080/01490457809377725.

Wada, E., T. Kadonaga, and S. Matsuo (1975), ^{15}N abundance in nitrogen of naturally occurring substances and global assessment of denitrification from isotopic viewpoint, *Geochem. J.*, *9*, 139–148.

Ward, P. D., J. W. Haggart, E. S. Carter, D. O. Wilbur, H. W. Tipper, and T. Evans (2001), Sudden productivity collapse associated with the Triassic-Jurassic boundary mass extinction, *Science*, *292*(5519), 1148–1151, doi:10.1126/science.1058574.

Weedon, G. P. (1986), Hemipelagic shelf sedimentation and climatic cycles: The basal Jurassic (Blue Lias) of south Britain, *Earth Planet. Sci. Lett.*, *76*(3–4), 321–335, doi:10.1016/0012-821X(86)90083-X.

Weedon, G. P. (1999), Astronomical calibration of the Jurassic time-scale from cyclostratigraphy in British mudrock formations, *Philos. Trans. R. Soc. London A*, *357*(1757), 1787–1813.

Whittaker, A., and G. W. Green (1983), Geology of the country around Weston-super-Mare: Memoir for 1:50,000 geological sheet 279, new series, with part of sheets 263 and 295, Her Majesty's Stn. Off., London.

Wignall, P. B. (2001a), Large igneous provinces and mass extinctions, *Earth Sci. Rev.*, *53*(1–2), 1–33, doi:10.1016/S0012-8252(00)00037-4.

Wignall, P. B. (2001b), Sedimentology of the Triassic-Jurassic boundary beds in Pinhay Bay (Devon, SW England), *Proc. Geol. Assoc.*, *112*(4), 349–360.

Williford, K. H., P. D. Ward, G. H. Garrison, and R. Buick (2007), An extended organic carbon-isotope record across the Triassic-Jurassic boundary in the Queen Charlotte Islands, British Columbia, Canada, *Palaeogeogr. Palaeoclimatol. Palaeoecol.*, *244*(1–4), 290–296, doi:10.1016/j.palaeo.2006.06.032.

Wilson, D. (1990), *Geology of the South Wales Coalfield*, Bernan, Blue Ridge Summit, Pa.